This article was downloaded by:
On: *25 January 2011*
Access details: *Access Details: Free Access*
Publisher *Taylor & Francis*
Informa Ltd Registered in England and Wales Registered Number: 1072954 Registered office: Mortimer House, 37-41 Mortimer Street, London W1T 3JH, UK

Separation Science and Technology
Publication details, including instructions for authors and subscription information:
http://www.informaworld.com/smpp/title~content=t713708471

Use of a Rotating Filter to Enhance Ceramic Membrane Filtration Performance of Latex Dispersions

Petr Mikulášek[a]; Petr Doleček[a]
[a] DEPARTMENT OF CHEMICAL ENGINEERING, UNIVERSITY OF CHEMICAL TECHNOLOGY, PARDUBICE, CZECH REPUBLIC

To cite this Article Mikulášek, Petr and Doleček, Petr(1994) 'Use of a Rotating Filter to Enhance Ceramic Membrane Filtration Performance of Latex Dispersions', Separation Science and Technology, 29: 15, 1943 — 1956
To link to this Article: DOI: 10.1080/01496399408002182
URL: http://dx.doi.org/10.1080/01496399408002182

PLEASE SCROLL DOWN FOR ARTICLE

Full terms and conditions of use: http://www.informaworld.com/terms-and-conditions-of-access.pdf

This article may be used for research, teaching and private study purposes. Any substantial or systematic reproduction, re-distribution, re-selling, loan or sub-licensing, systematic supply or distribution in any form to anyone is expressly forbidden.

The publisher does not give any warranty express or implied or make any representation that the contents will be complete or accurate or up to date. The accuracy of any instructions, formulae and drug doses should be independently verified with primary sources. The publisher shall not be liable for any loss, actions, claims, proceedings, demand or costs or damages whatsoever or howsoever caused arising directly or indirectly in connection with or arising out of the use of this material.

SEPARATION SCIENCE AND TECHNOLOGY, **29**(15), pp. 1943–1956, 1994

Use of a Rotating Filter to Enhance Ceramic Membrane Filtration Performance of Latex Dispersions

PETR MIKULÁŠEK* and PETR DOLEČEK
DEPARTMENT OF CHEMICAL ENGINEERING
UNIVERSITY OF CHEMICAL TECHNOLOGY
NÁM. ČS. LEGIÍ 565, 532 10 PARDUBICE, CZECH REPUBLIC

Downloaded At: 12:11 25 January 2011

ABSTRACT

The performances of both the tangential crossflow system and the rotating system with a tubular microfiltration ceramic membrane were investigated experimentally in the separation of latex dispersions. In addition, the shear rate at the membrane surface for azimuthal flow in an annulus with a porous wall on the rotating inner cylinder was solved for the narrow-gap approximation. In contrast to the tangential crossflow system, the rotary system was characterized by a significantly higher flux. The increase in the membrane flux was achieved at shear rates less than those for the crossflow system investigated.

INTRODUCTION

The use of inorganic membranes in separation technologies is relatively new and has given rise to much interest in recent years. For this reason the major types of ceramics used in ceramic membrane manufacturing consist of refractory oxides: alumina, zirconia, or titania. Ceramic membranes exhibit unique physical and chemical properties which are only partially shown (or are completely absent) by polymeric membranes. For example, they can be used at significantly higher temperatures, have better structural stability without the problems of swelling or compaction, generally can withstand more harsh chemical environments, are not subject to microbiological attack, and can be backflushed, steam sterilized,

* To whom correspondence should be addressed.

Copyright © 1994 by Marcel Dekker, Inc.

or autoclaved. Ceramic membranes represent a distinct class of inorganic membranes. Other classes consist of membrane materials such as glasses, carbon and metals, and organic-inorganic polymers (1).

Membrane filtration processes are currently mostly used in the production of ultrapure water, the processing of food and dairy products, the recovery of electrodeposition paints, the treatment of oil and latex dispersions, and in biotechnology-oriented applications. However, the present membrane processes for liquid feed streams are complicated by the phenomena of membrane fouling and of concentration polarization in the liquid boundary layer adjacent to the membrane wall. Concentration polarization and membrane fouling are major concerns in the successful use of membrane-based separation operation in a crossflow mode, as their net effect is to reduce the permeate flux, thereby resulting in less productivity. Such limitations have spurred research into the utilization of novel hydrodynamic approaches in membrane separation systems and the development of new membrane materials.

Downloaded At: 12:11 25 January 2011

Most of the rotating membrane filters, which consist of a pair of concentric cylinders with the inner one rotating and the outer one stationary, have been commercialized. Above a well-defined angular velocity (which depends on curvature, gap size, and fluid properties), the azimuthal flow becomes unstable and forms so-called "Taylor vortices." Thus, besides the high wall shear rate, the secondary flow consisting of the regular toroidal vortices rotating inside the annulus is established. If a membrane is placed on the outside of the rotating surface inside of this equipment, the vortices may efficiently reduce the extent of concentration polarization by creating excellent mixing normal to the membrane surface. As the angular velocity is increasing above its critical value, the degree of mixing intensifies, further improving the efficiency of this filtration scheme. Thus, the membrane can be used more efficiently, leading to a smaller membrane area requirement.

This type of filter has been tested in three major areas of downstream processing in biotechnology—clarification, cell harvesting, and protein concentration (2–8)—and has been used to filter suspensions and emulsions with very difficult rheological properties (9–17).

Mateus and Cabral (6) used a rotary membrane system in the downstream processing of fermentation media. Their results clearly show the best performance of the rotary membrane system when compared with hollow fibers and plate-and-frame modules. Belfort et al. (8) measured the permeation rates of deionized water, fetal bovine serum medium, and a commercial serum-free medium through microfiltration and ultrafiltration membranes. Their results indicate that the centrifugal force acts both on the fouling material and on the fluid, causing an increase and a decrease

in the wall flux, respectively. The experimental results suggest that the former effect dominates in this case. Mikulášek et al. (16) and Belfort et al. (17) studied the microfiltration of a dilute suspension of well-defined spherical particles using a rotating annular filter with a view to understanding the effect of transmembrane pressure on flux and the mechanism of fouling. They suggest that particle intrusion into the pores of the membrane, thereby causing pore constriction and plugging, is the dominant form of fouling. Particle intrusion depends on membrane pore size distribution, density difference between the particles and the carrying fluid, particle size, and rotational speed.

Although numerous studies on latex ultrafiltration or microfiltration using polymeric membranes and standard crossflow systems have been reported in the literature (18–24), relatively few reports have been made on the use of ceramic membranes (e.g., Refs. 25–29). On the other hand, many attempts have been made to utilize a rotating module for filtration of emulsions and suspensions (9–17). Indeed, it has been assumed that the action of Taylor vortices generated in these types of rotational shear-filters contributes to improved mass-transfer, but no detailed testing of this device seems to have been published. We therefore decided to investigate the concept of microfiltration by a rotating membrane device, focusing our interest on the influence of shear rate in ceramic microfiltration of latex dispersions.

Downloaded At: 12:11 25 January 2011

SHEAR RATE AT THE ROTATIONAL MEMBRANE SURFACE

In another paper (30) we analyzed the mathematical model of pure fluid flow in a rotary filtration module. The rotary filtration module is depicted in Fig. 1. The feed flows along the z-axis in the annular gap between two concentric cylinders, the inner one with a porous membrane and rotating while the outer one is impermeable and stationary. Permeate flows radially inward through the membrane and is collected by a duct along the axis of rotation. The validity of the model is restricted to the region without Taylor vortices. The axial velocity component u_z is taken to be that of flow through the annulus with both cylindrical surfaces impermeable. The radial velocity u_r has been determined from the continuity equation in an analytical form. The azimuthal velocity u_θ and pressure are obtained from θ- and r-components of Navier–Stokes equations, respectively. The calculations were performed for the parameters $\beta = R_1/R_2$ in the range from 0.5 to 0.99 and $\mathrm{Re}_r = \rho q/\mu$ from 0 to 800.

Here we extend the analysis with calculations of the shear rate at the membrane surface. The shear rate tensor has four nonzero components

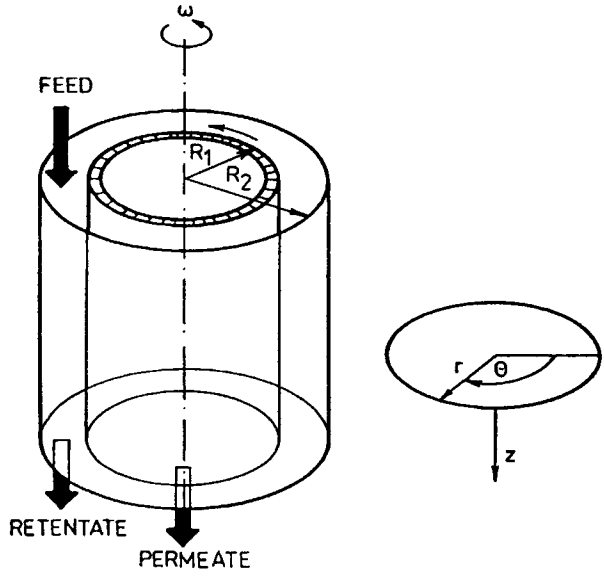

FIG. 1 Coordinates for the rotary filtration system.

Downloaded At: 12:11 25 January 2011

for the system in question, but for higher ω the $r\theta$-component will usually prevail. Because of the symmetry along the z-axis, all variables are independent of the azimuthal coordinate. Then the $r\theta$-component of shear rate tensor can be expressed in the form

$$\dot{\gamma}_{r\theta} = r\frac{\partial}{\partial r}\left(\frac{u_\theta}{r}\right) \tag{1}$$

If the surface of inner cylinder is impermeable ($Re_r = 0$), it can be shown (31) that

$$\dot{\gamma}_{r\theta,0} = \dot{\gamma}_{r\theta}(Re_r = 0) = -\frac{2\omega}{1-\beta^2}\frac{R_1^2}{r^2} \tag{2}$$

$$\dot{\gamma}_{r\theta,0}(R_1) = -\frac{2\omega}{1-\beta^2} \tag{3}$$

For increasing values of Re_r, the drop of azimuthal velocity u_θ with the radial coordinate near the membrane surface becomes more pronounced and the magnitude of $\dot{\gamma}_{r\theta,0}(R_1)$ increases. Using dimensionless variables:

$$r_b = r/R_2, \qquad u_{rb} = u_r R_2/q, \qquad u_{\theta b} = u_\theta/(\omega R_1) \tag{4}$$

we can express the $r\theta$-component of shear rate as follows:

$$\dot{\gamma}_{r\theta} = \omega\beta r_b \frac{\partial}{\partial r_b}\left(\frac{u_{\theta b}}{r_b}\right) = \omega\beta\left(Y - \frac{2u_{\theta b}}{r_b}\right) \tag{5}$$

where Y is defined (30) as

$$Y = \frac{1}{r_b}\frac{\partial}{\partial r_b}(r_b u_{\theta b}) \tag{6}$$

Then the shear rate at the membrane surface can be expressed as

$$\dot{\gamma}_{r\theta}(R_1) = \omega\beta\left(Y(\beta) - \frac{2}{\beta}\right) \tag{7}$$

where

$$Y(\beta) = Y(1)\exp(-\mathrm{Re}_r\int_\beta^1 u_{rb}\,dr_b) \tag{8}$$

$$u_{rb}(r_b, \beta) = -\frac{1}{2\pi r_b}\frac{(1 - r_b^2)^2 + \dfrac{1 - \beta^2}{\ln(\beta)}[1 - r_b^2 + 2r_b^2\ln(r_b)]}{1 - \beta^4 + \dfrac{(1 - \beta^2)^2}{\ln(\beta)}} \tag{9}$$

$$\int_\beta^1 u_{rb}\,dr_b = \frac{1}{2\pi}\frac{\dfrac{(1 - \beta^2)^2}{\ln(\beta)} + \ln(\beta) + \dfrac{5\beta^4}{4} - \beta^2 - \dfrac{1}{4}}{1 - \beta^4 + \dfrac{(1 - \beta^2)^2}{\ln(\beta)}} \tag{10}$$

$$Y(1) = -\frac{\beta}{\int_\beta^1 r_b \exp(-\mathrm{Re}_r\int_{r_b}^1 u_{rb}\,dr_b')\,dr_b} \tag{11}$$

The results of calculations are demonstrated in Fig. 2. Dimensionless variable $\dot{\gamma}_{r\theta}(R_1)/\dot{\gamma}_{r\theta,0}(R_1)$ is plotted versus radial Reynolds number Re_r for several values of ratio β. We can see that the shear rate increases linearly with increasing Re_r. The slope of the straight lines increases with β increasing.

EXPERIMENTAL

Membranes

The ceramic membranes studied in this work were asymmetric alumina membranes (Terronic, Czech Republic). They were configured as single cylindrical tubes 0.1 m long, 6 mm i.d. and 10 mm o.d. (for crossflow

Downloaded At: 12:11 25 January 2011

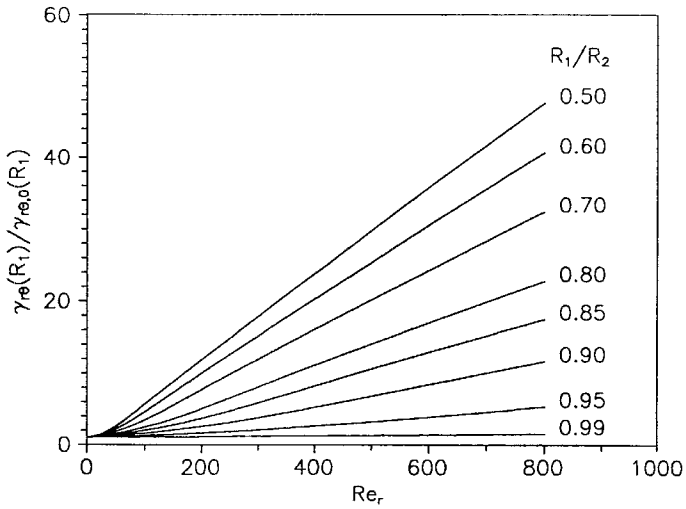

FIG. 2 The relative shear rate as a function of permeate Reynolds number for different radius ratios, $\beta = R_1/R_2$.

Downloaded At: 12:11 25 January 2011

system), and 12 mm i.d. and 17 mm o.d. (for rotating system), consisting of a thin α-alumina layer on the top of a support. The pore size distribution of the membrane used is shown in Fig. 3. The liquid displacement method was used for the distribution determination (32).

Feeds

Five different feeds were used either with the crossflow or the rotational systems to determine the effect on flux. The first was deionized water (reverse osmosis, ion exchange), and the next four were dilute latex dispersions of poly(vinyl acetate) and acrylic copolymer in deionized water. The concentration of the dispersions were 1% (w/w) solids.

Equipment

The microfiltration studies were carried out in a crossflow filtration unit and in a rotating filtration unit equipped with ceramic membranes.

The crossflow filtration unit was same as in Reference 33. Latex dispersions were circulated through the module by a piston pump. The unit allowed studies in which the transmembrane pressure and the crossflow velocity were independently varied.

The rotating filtration system is shown in Fig. 4. The filter consisted of an outer, transparent, acrylic-resin cylinder; an inner, rotating, ceramic

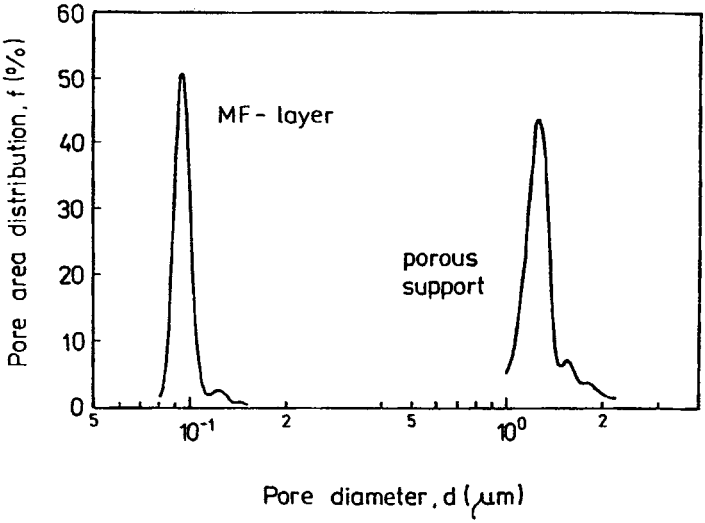

FIG. 3 Pore size distribution of the microfiltration layer, and porous support of alumina microfiltration membrane used.

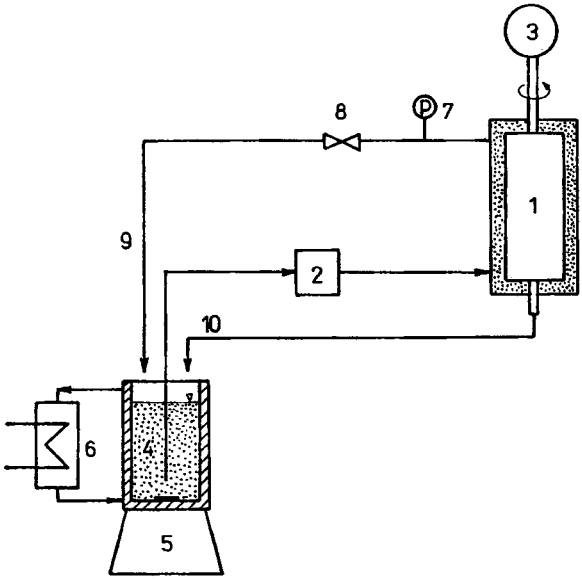

FIG. 4 Schematic diagram of the rotating filtration apparatus: (1) rotating cylinder; (2) pump; (3) motor; (4) beaker with dispersion; (5) magnetic stirrer; (6) heat exchanger; (7) pressure transducer; (8) valve; (9) retentate flow; (10) permeate flow.

Downloaded At: 12:11 25 January 2011

membrane cylinder; and a flange. The inner cylinder contained an alumina ceramic membrane with a length of 0.1 m, an effective area of 20 cm^2, and a mean pore diameter of 0.1 μm. The feed was pumped into the annular gap formed by two cylinders. The mean transmembrane pressure in the annular gap was monitored by regulating a simple valve which creates a backpressure along the membrane to the outlet of the pump. The pressure was measured at the wall of the outer cylinder of the filtration unit. The design and operating details of the rotating filter are summarized in Table 1.

RESULTS AND DISCUSSION

Crossflow Microfiltration

Analysis of the permeate showed complete rejection of the latex particles in the feed. Therefore, the ceramic membranes used for our experiments are acceptable for microfiltration of the latexes studied.

The flux during microfiltration of the latexes was substantially lower than that of the pure water flux, ranging from 0.2 to 30% of the water flux, indicating cake (gel) or pore blocking control in all the experiments.

In the majority of cases the experimental data showed a trend toward higher fluxes for acrylic copolymer latexes compared with poly(vinyl acetate) latexes. The lowest flux was exhibited by a poly(vinyl acetate) latex manufactured without any additives and with only a protective colloid [poly(vinyl alcohol)]. Therefore, this latex dispersion has poor mechanical stability during microfiltration because the protective colloid may be stripped from the surface of the polymer particle when latex becomes waste upon dilution. Simultaneously, a more stable flux was obtained for polyvinyl acetate paint (see Fig. 5). In this case the latex paint stability can be improved by the presence of physically adsorbed nonionic polymer chains on the surface of the particles, by complete interaction between the particular latex–surfactant combination, and by the pigments and filling agents content.

TABLE 1
Design and Operating Details of the Rotating Membrane System

Radius of rotating cylinder	8.5×10^{-3} m
Annular gap width	1.5×10^{-3} m
Membrane cartridge length	0.10 m
Effective membrane surface area	2×10^{-3} m^2
Operational pressure range	0–200 kPa
Angular velocity range	0–365 $rad \cdot s^{-1}$

Downloaded At: 12:11 25 January 2011

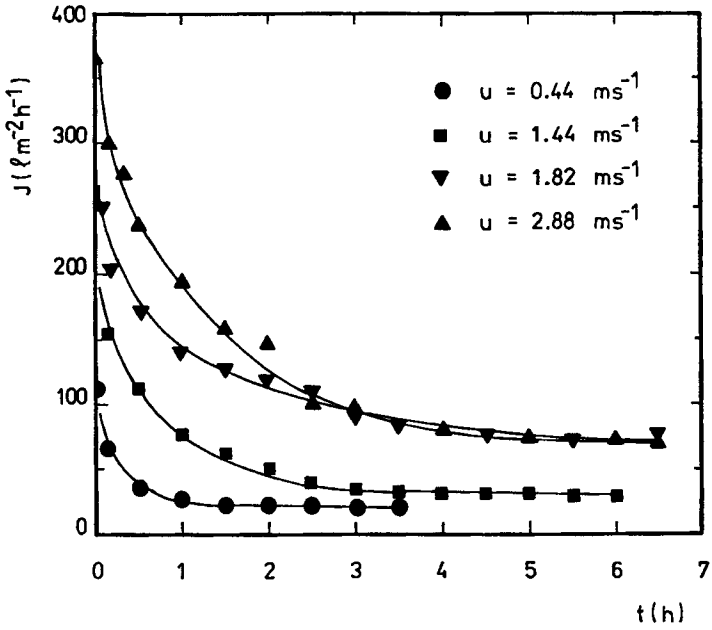

FIG. 5 Permeate flux versus time for latex dispersion crossflow microfiltration. Concentration, 1% solids; transmembrane pressure, 100 kPa.

Downloaded At: 12:11 25 January 2011

It follows from Fig. 5 that as the filtration process continues, the filtration rate gradually decreases. As a result, the drag force on the solutes which constitute the gel–cake decreases. Consequently, the gel–cake begins to be swept away, and then the filtration rate tends to approach a plateau or dynamically balanced value. This quasi-steady rate increases with crossflow velocity (29).

Rotational Microfiltration

The wall flux of deionized water and acrylic latex dispersions through a microfiltration membrane were measured to test the results of the mathematical analysis. A laboratory rotating filter with the ceramic microfiltration membrane on the inner rotating cylinder was used.

For a fixed angular velocity, onset of flux will occur when the transmembrane pressure exceeds the outward radial liquid pressure induced by centrifugal force (4, 16, 17). The centrifugal pressure is proportional to the square of the rotational speed (8, 16, 17), but depends on the Taylor flow conditions, too.

The influence of transmembrane pressure and angular velocity on the flux was studied with dilute latex dispersions in a recycle mode. Figure 6 shows the results of these experiments. As generally is the case in crossflow filtration of latex dispersions, asymptotic curves of flux versus pressure are obtained with different levels depending on the angular velocity. On the basis of Fig. 6 we speculate that the resistance to flow through the gel–cake is dependent on transmembrane pressure (through compressibility, for example) and inversely dependent on angular velocity (through a balance between convective drag to the membrane and inertial lift, shear-induced diffusion, and centrifugal force away from the membrane).

The dominant influence of the angular velocity was studied by separate experiments under constant-pressure conditions. In all cases a substantial decrease of cake resistance with increasing angular velocity is observed. These results confirm previous conclusions based on previous rotating filter experiments (16, 17). This cannot be achieved simply with a stationary membrane in the crossflow filtration system because a shear rate increase due to increasing the flow leads to a rise in pressure drop and therefore a decrease of transmembrane pressure.

Downloaded At: 12:11 25 January 2011

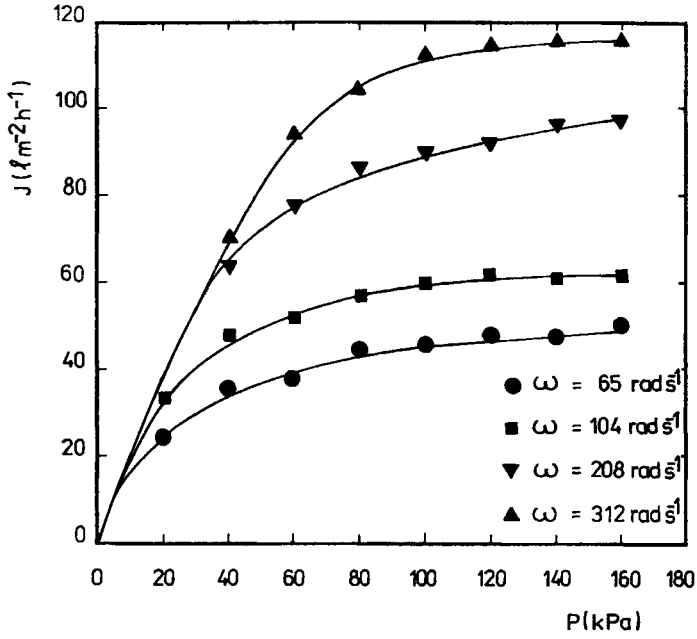

FIG. 6 Permeate flux versus actual transmembrane pressure for latex dispersion rotational microfiltration at different angular velocities. Concentration, 1% solids.

A more extensive study of the effect of a shear rate on flux was made in studies comparing the steady-state flux of tangential crossflow and rotary systems. Steady-state flux was defined as the average flux measured after a rapid decline in the flux upon initial pressurization. To facilitate comparison between the two different flow configurations, a shear rate at the membrane surface, assuming Newtonian fluid behavior, was determined for the tube crossflow system from

$$\dot{\gamma} = 8u/d \tag{12}$$

and for the rotating system from Fig. 2 and Eq. (3).

As shown in Fig. 7, the steady-state flux in the rotary system was approximately linear with the shear rate at the membrane surface; the flux had not reached a maximum at $\omega = 365$ rad·s^{-1}, the maximum angular velocity of the prototype. This result can be realized by assuming that deposited particles remain on the membrane when a friction force proportional to the transmembrane pressure exceeds the drag from the shear rate. In contrast, the flux in the crossflow system was nearly constant with increasing crossflow rate above a shear rate of approximately 3000 s^{-1} at the membrane surface.

It follows from Fig. 7 that at conditions yielding identical shear rates, the membrane flux in the rotary system is approximately twice that observed in the crossflow system. A three- to fourfold higher shear rate was

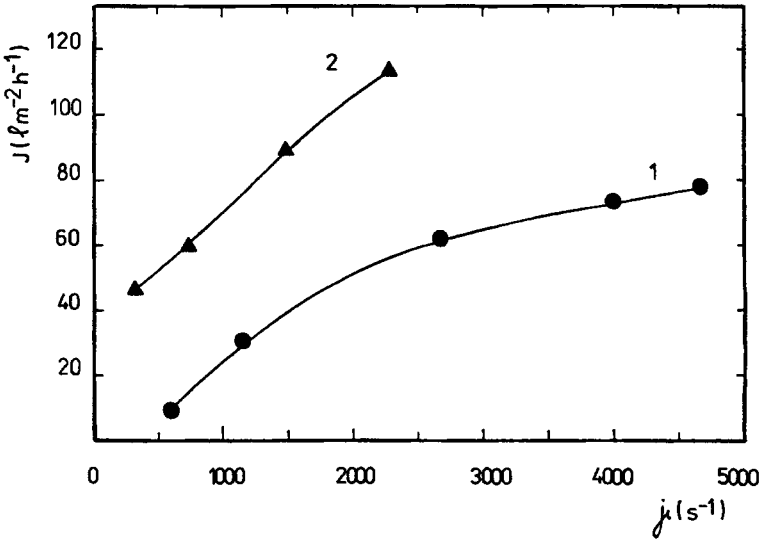

FIG. 7 Steady-state dispersion flux as a function of shear rate: (1) crossflow system; (2) rotating system. Concentration, 1% solids; transmembrane pressure, 100 kPa.

Downloaded At: 12:11 25 January 2011

required in the crossflow system to achieve the same membrane flux as in the rotary system.

CONCLUSIONS

The microfiltration of dilute dispersions of various types of latexes was studied using a crossflow unit and a rotating annular filter equipped with alumina ceramic membranes.

The wall flux of deionized water and latex dispersions through a microfiltration membrane increased as the rotational speed (i.e., the angular velocity) of the filter was increased. Both the shear rate and centrifugal force on a sphere in the annular gap of the filter enhanced the reduction of membrane fouling.

The superior hydrodynamics of the rotary membrane filtration result in permeate fluxes several times higher than for a crossflow filtration system with a tubular membrane. Therefore, the concept of dynamic microfiltration through a rotating membrane looks attractive because: 1) it permits uncoupling of the wall shear rate from the tangential flow and allows very high shear rates to be obtained at low feed flows; 2) the intrinsically higher flux of rotary systems reduces the required time of contact of the feed fluid with the membrane surface and enables a smaller membrane area to be used to achieve a specified flow rate.

Downloaded At: 12:11 25 January 2011

NOTATION

d	inner diameter of the membrane tube (m)
J	permeate flux ($L \cdot m^{-2} \cdot h^{-1}$)
P	actual transmembrane pressure (Pa)
q	permeate flux per unit of length ($m^2 \cdot s^{-1}$)
r	radial coordinate (m)
R_1	radius of the outer membrane surface (m)
R_2	inner radius of the outer cylinder (m)
Re_r	permeate Reynolds number ($= q/\nu$)
u	velocity ($m \cdot s^{-1}$)
u_r, u_θ, u_z	radial, azimuthal, and axial velocity components ($m \cdot s^{-1}$)
z	axial coordinate (m)

Greek Symbols

β	ratio R_1/R_2
$\dot{\gamma}$	shear rate (s^{-1})
θ	azimuthal coordinate

μ dynamic fluid viscosity (Pa·s)
ν kinematic viscosity ($m^2 \cdot s^{-1}$)
ρ fluid density ($kg \cdot m^{-3}$)
ω angular velocity of the inner cylinder ($rad \cdot s^{-1}$)

Subscript

b dimensionless variable

REFERENCES

1. R. R. Bhave, *Inorganic Membranes*, Van Nostrand Reinhold, New York, 1991.
2. B. Hallström and M. Lopez-Leiva, *Desalination*, *24*, 273 (1978).
3. K. H. Kroner, V. Nissinen, and H. Ziegler, *Biol Technology*, *5*, 921 (1987).
4. K. H. Kroner and V. Nissinen, *J Membr. Sci.*, *36*, 85 (1988).
5. P. M. Rolchigo, W. A. Raymond, and J. Hildebrandt, *Process Biochem.*, *24*, supplement iii–vii (1989).
6. M. Mateus and J. M. S. Cabral, *Biotechnol. Tech.*, *5*, 43 (1991).
7. U. B. Holeschovsky and C. L. Cooney, *AIChE J.*, *37*, 1219 (1991).
8. G. Belfort, J. M. Pimbley, A. Greiner, and K. Y. Chung, *J. Membr. Sci.*, *77*, 1 (1993).
9. W. Tobler, *Filtr. Sep.*, *19*, 329 (1982).
10. F. Vigo, C. Uliana, and P. Lupino, *Sep. Sci. Technol.*, *20*, 213 (1985).
11. F. Vigo and C. Uliana, *Ibid.*, *21*, 367 (1986).
12. A. Rushton and G. S. Zhang, *Desalination*, *70*, 379 (1988).
13. M. Y. Jaffrin, *J. Membr. Sci.*, *44*, 115 (1989).
14. G. Beaudoin and M. Y. Jaffrin, *Artif. Organs*, *13*, 43 (1989).
15. T. Murase, E. Iritami, P. Chidphong, K. Kano, K. Atsumi, and M. Shirato, *Int. Chem. Eng.*, *27*, 304 (1991).
16. P. Mikulášek, J. M. Pimbley, and G. Belfort, Symposium on Engineering of Membrane Processes, Garmisch-Partenkirchen, 1992.
17. G. Belfort, P. Mikulášek, J. M. Pimbley, and K. Y. Chung, *J. Membr. Sci.*, *77*, 23 (1993).
18. M. C. Porter, *Ind. Eng. Chem., Prod. Res. Dev.*, *11*, 234 (1972).
19. J. Zahka and L. Mir, *Chem. Eng. Prog.*, *73*, 53 (1977).
20. J. J. S. Shen, *Ultrafiltration of Industrial Latex Streams: Data, Analysis and Design*, Paper presented at the 88th AIChE National Meeting, Philadelphia, 1980.
21. R. Roullet, "Ultrafiltration of Latex Emulsion. North Western Branch Papers," *Inst. Chem. Eng.*, *4*, 7.1–7.4 (1980).
22. D. Kirjassof, W. R. Grace, S. Pinto, and C. Hoffman, *Chem. Eng. Prog.*, *76*, 58 (1980).
23. J. J. S. Shen and L. Mir, *Ind. Eng. Chem., Prod. Res. Dev.*, *21*, 63 (1982).
24. M. S. Suwandi and M. S. Lefebvre, *Desalination*, *70*, 225 (1988).
25. G. M. Rios, H. Rakotoarisoa, and B. Tarodo de la Fuente, *J. Membr. Sci.*, *34*, 331 (1987).
26. Y. Matsumoto, S. Nakao, and S. Kimura, *Int. Chem. Eng.*, *28*, 677 (1988).
27. W. M. Clark, A. Bansal, M. Sontakke, and Y. H. Ma, *J. Membr. Sci.*, *55*, 21 (1991).
28. F. René and M. Lalande, *Ibid.*, *56*, 29 (1991).
29. P. Mikulášek, *Rec. Prog. Genie Procedes*, *6*(22), 305 (1992).
30. P. Doleček, P. Mikulášek, and G. Belfort, "The Performance of a Rotating Filter. 1.

Downloaded At: 12:11 25 January 2011

Theoretical Analysis of the Flow in an Annulus with a Rotating Inner Porous Wall," *J. Membr. Sci.*, In Press.
31. V. Sinevic, R. Kuboi, and A. W. Nienow, *Chem. Eng. Sci.*, *41*, 2915 (1986).
32. P. Mikulášek and P. Doleček, *Sep. Sci. Technol.*, *29*, 1183 (1994).
33. P. Mikulášek and J. Cakl, *Desalination*, *95*, 211 (1994).

Received by editor February 3, 1994

Downloaded At: 12:11 25 January 2011